Desalination and Water Treatment
www.deswater.com

doi: 10.5004/dwt.2018.21779

101 (2018) 301–312
January

Preparation of chitin with different degrees of deacetylation from crab shells waste and its application in the removal of Congo Red

Neng Fan, Liu-Qin Ge*, You-Zhou Zhou, Mei-Sheng Xia

Department of Marine Science, Ocean College, Zhejiang University, Zhoushan 316021, China, Tel. +86 13758246689; email: gliuqin@163.com (L.-Q. Ge), Tel. +86 17682300729; email: fanneng@zju.edu.cn (N. Fan), Tel. +86 18627953033; email: 21534038@zju.edu.cn (Y.-Z. Zhou), Tel. +86 13958197388; email: msxia@zju.edu.cn (M.-S. Xia)

Received 24 July 2017; Accepted 8 December 2017

ABSTRACT

Chitin adsorbents with different degrees of deacetylation (DDA) were prepared from crab shells waste and applied in adsorptive removal of dye Congo Red (CR). The adsorbents were characterized by thermal gravimetric analysis, Fourier transform infrared spectroscopy, X-ray diffraction, and elemental analysis. The effects of solid–liquid ratio, initial dye concentration, contact time, temperature, pH value, salt concentration, and DDA on adsorption were studied. It was indicated from orthogonal experiments that the removal of CR reached 99.28% under the optimum condition (DDA = 17.85%, pH = 5.40, and time = 20 h) at 300 K. The equilibrium data were plotted by Langmuir and Freundlich isotherms and described better with Langmuir model (Q_m = 366.3 mg/g, 300 K) as the temperature increased and the adsorption kinetics was well fitted by pseudo-second-order equation. It was verified from the thermodynamic parameters (ΔG, ΔH, and ΔS) that the adsorption was spontaneous, exothermic and entropy decreasing. Functional groups including amino, acetyl amino, O-glycosides, and –O– on the pyranose ring of chitin were involved in adsorption as active sites through van der Waals force and hydrogen-bonding with the adsorbate. Moreover, CR adsorption on chitin with different DDA further revealed that the crystallinity of chitin played a more important role than amino group content.

Keywords: Chitin; DDA; Crab shell; Congo Red; Adsorption

1. Introduction

The wide use of dyes in modern industries such as textile, dyeing, leather, printing, paper, plastics, food, and cosmetic has drawn increasing attention to the environmental contamination issue. At a rough estimate, up to 70,000 tons of dyestuffs are directly discharged without treatment process in the world every year [1]. Most dyestuffs especially synthetic dyestuffs can hardly be degraded by bacteria or other microorganisms in the nature because of their stable structures. It is well known that dye containing water could reduce sunlight penetration into the water and thus inhibit the photosynthesis process of aquatic plants [2]. Additionally, synthetic dyes may also have potential hazards associated with the carcinogenic, allergenic, mutagenic, and toxic natures [3], making them harmful to aquatic organisms and human beings. Among these dyes, Congo Red (CR) (disodium 3,3′-[biphenyl-4,4′-diyldi(*E*)diazene-2,1-diyl] bis(4-aminonaphthalene-1-sulfonate)) is a common benzidine-based anionic diazo dye with the advantage of substantivity. In other words, CR could dye cellulose fiber (cotton, linen, etc.) or protein fiber (wool, silk, etc.) without other medium. However, it can be metabolized to benzidine, a known human carcinogen [4]. For this reason, removal of CR from wastewater effluents is of a significant and practical importance.

* Corresponding author.

In recent years, many physicochemical methods have been applied in dyestuff effluents treatment, for instance, coagulation/flocculation [5], oxidation [6], electrolysis [7], membrane filtration [8], ion-exchange [9], biotechnology [10], adsorption [11–13], etc. Most of these are considered to be unpractical because of high cost or low efficiency, while adsorption is regarded as an efficient and economic method. Quantities of materials have been developed as adsorbents, such as activated carbon [14], sawdust [15], rice hull [16], wheat straw [17], red mud [18], fly ash [19], coconut coir pith [20], kaolin [21], bentonite [22], chitosan–Fe(III) [23], etc.

Many researchers have been trying to explore a kind of adsorbent with high adsorption capacity and low price. For example, Foroughi-Dahr et al. [24,25] carried out abundant researches on the removal of CR by employing tea waste (TW) as a low-cost adsorbent. The results showed that vibratory mill treatment leads to an increase in the adsorption capacity of TW from 32.26 to 43.48 mg/g and the cetyltrimethylammonium bromide (CTAB)-modified TW exhibited a relatively high adsorption capacity of 106.4 mg/g. In recent years, some researchers focus their attention on chitin, β-(1,4)-2-acetamido-2-deoxy-ᴅ-glucose, which is the second most abundant polysaccharide biopolymer after cellulose on the earth. It is estimated that at least 100 billion tons of chitin is synthesized and over 150,000 tons is commercially available in the nature every year [26]. There are three types of chitin: α-chitin, β-chitin, and γ-chitin. α-chitin, which is widely distributed in insects, crabs, lobsters, and shrimps, is the most abundant and stable form of chitin [27]. Due to its rigid structure and anti-parallel molecular chains, α-chitin has strong intra- and inter-molecular hydrogen bonds. Chitin has a relatively high adsorption capacity and low cost, and as a biopolymer, it is biodegradable, biocompatible, renewable, and non-toxic. Therefore, chitin has become an attractive biosorbent for various kinds of dyes. Sismanoglu and Aroguz [3] reported that chitin showed the maximum uptake percentage for diazo dye Trypan Blue compared with pyrolyzed petrified sediment and pyrolyzed sawdust from maple bark. Zúñiga-Zamora et al. [28] investigated the CR removal by chitin extracted from shrimp exoskeleton and found that under the optimum conditions determined by respond surface method, chitin exhibited a relatively high adsorption capacity than other low-cost adsorbents such as cattail root, bamboo dust carbon, and banana peel. Franco et al. [29] modified the chitin surface by ultrasonic processor for methylene blue adsorption using the statistical physics theory, and it was concluded that the adsorption was mainly related to hydroxyl and *N*-acetyl groups on modified chitin. Besides, chitin composite adsorbent such as chitin/graphene oxide hybrid composite [1] was also prepared to improve its comprehensive adsorption performance. Since the degree of deacetylation (DDA) of chitin has a great effect on its solubility, crystallinity, reactivity, etc., it should also make a difference to dye adsorption, but no relative research on DDA has been reported up to now.

Large quantities of crab shells wastes are produced from the seafood processing industry [30]. The use of chitin prepared from crab shells for dye adsorption was hardly reported, and the adsorption mechanism has not been made clear yet. Thus, in this work, chitin was extracted from crab shells and further partially deacetylated for the removal of CR dye from aqueous solution. No additional grafting or coating procedure was introduced on account of environment protection and expense reduction. The adsorbents were characterized by thermal gravimetric analysis (TGA), Fourier transform infrared spectroscopy (FTIR), X-ray diffraction (XRD), elemental analysis, and UV–Vis spectroscopy. The adsorption experiment was carried out under varying factors including DDA, solid–liquid ratio, initial dye concentration, contact time, temperatures, pH values, and salt concentration, and the optimum condition was determined by Taguchi design method. It should be pointed out that the effect of DDA of chitin toward CR dye adsorption removal has not been researched based on our best knowledge. Furthermore, the adsorption equilibrium isotherm, dynamics, and thermodynamics were also studied.

2. Experimental

2.1. Materials

Crab shells waste was supplied by a seafood enterprise in Zhoushan, China, to prepare crab shells powder (CSP) and chitin with different DDA. Hydrochloric acid (AR) and sodium hydroxide (AR) were purchased from Sinopharm Chemical Reagent Co., Ltd. (China). CR of indicator grade was obtained from Aladdin Industrial Corporation (China). All these reagents were used without further purification.

2.2. Preparation of crab shells powder

Raw crab shells were washed with running water to remove the meat remnant, and then desiccated in an electrothermal oven at the temperature of 100°C for 12 h. After that, the dried crab shells were grounded by a small pulverizer into CSP with the mean diameter of ~55 μm.

2.3. Extraction of chitin

In this study, chitin was extracted from CSP through demineralization and deproteinization. In the first step, the CSP was mixed with 3% HCl solution at room temperature under stirring to remove calcium carbonate and calcium phosphate. Then, the mixture was filtered through 250 mesh size gauze and subsequently washed with deionized water until the filtrate was neutral. The crude product was dried in an electrothermal oven at 60°C overnight and then ground into powder. Second, the demineralized powder was mixed with 4% NaOH solution at 50°C under stirring for 24 h to remove organic substances such as proteins, fats, and pigments, then it was filtered by gauze, washed by deionized water till neutralization, and dried in the oven at 60°C overnight. After that, the chitin was crushed into powder and further dried in the oven at 100°C for 12 h. Finally, the chitin powder was obtained and named CT for further use.

2.4. Preparation of chitin with different degree of deacetylation

CT was deacetylated in NaOH solution with high concentration of 40%, in a w/v ratio of 1:5 at certain reaction conditions. After that, the mixtures were filtered and washed with deionized water until the pH was neutral. The products

Table 1
The degrees of deacetylation (DDA) of chitin prepared under different deacetylation conditions

Sample	NaOH concentration (%)	Reaction temperature (°C)	Reaction time (h)	C/N	DDA (%)
CT	–	–	–	6.841	0.93
CT-1	40	80	0.5	6.824	1.93
CT-2	40	80	1	6.776	4.73
CT-3	40	90	2	6.651	12.02
CT-4	40	90	4	6.551	17.85
CT-5	40	90	4 + 4	6.146	41.48

were dried in the oven at 60°C overnight, crushed into powder and further dried at 100°C for 12 h. The deacetylation reactions were carried out under the following conditions: (1) 80°C, 0.5 h; (2) 80°C, 1 h; (3) 90°C, 2 h; (4) 90°C, 4 h; and (5) 90°C, 4 h, twice, and the resulted chitins with different DDA were named as CT-1, CT-2, CT-3, CT-4, and CT-5, respectively (Table 1).

2.5. Characterization

2.5.1. Elemental analysis

Since the low-DDA chitin is insoluble in water solution or most organic solvents, methods such as acid–base titration, potentiometric titration and UV–Vis spectrophotometry, cannot be applied to the measurement of its DDA. In this paper, elemental analysis was adopted for DDA determination, performed on Vario Micro elemental analyzer (Elementar Analysensysteme GmbH, Germany). The DDA was calculated from C, H, and N content by the following equation:

$$\text{DDA \%} = (6.857 - (\text{C/N}))/1.714 \times 100\% \quad (1)$$

where C/N represents the ratio of carbon and nitrogen content estimated by elemental analysis, 6.857 is the theoretical ratio of carbon and nitrogen content in fully acetylated chitin, and 1.714 is the C/N difference between fully acetylated chitin and fully deacetylated chitin.

2.5.2. Thermal gravimetric analysis

The thermal stability of CSP, CT, and CT-5 was measured on a TA-Q500 thermogravimetric analyzer (TA, America) under heating rate of 10°C/min and data collecting rate of 120 points/K. The test temperature range was 50–1,000°C for CSP, and 50–650°C for CT and CT-5. All tests were under 60.0 mL/min dynamic nitrogen atmosphere. Before test, the samples were heated from ambient temperature to 100°C and remained at 100°C for 5 min to remove the moisture.

2.5.3. Fourier transform infrared spectroscopy

The FTIR was performed by using a Nicolet iS50 FT-IR Spectrometer (Nicolet, America). All samples were measured with the wavenumber range of 4,000–400 cm^{-1}, and 16 scans at a resolution of 8 cm^{-1}.

2.5.4. X-ray diffraction

XRD data of CSP, CT, and CT-5 were collected by Shimadzu XRD-6000 diffractometer (Shimadzu, Japan) with a Cu Kα radiation, generator voltage of 40 kV, and tube current of 40 mA. The scan range (2θ) was 5°–80°, with a step size of 0.026° and counting time of 24 s per step.

2.6. Adsorption equilibrium study

A series of CR adsorption experiments were carried out by agitating 0.1 g of the absorbent with 30 mL of dye solution in a plastic tube using a temperature-controlled shaker at a speed of 200 rpm. Various concentrations of CR dye solutions were prepared using deionized water. The pH value was adjusted by 0.1 M HCl or 0.1 M NaOH solution. The effect of salt concentration was studied by adding NaCl or Na_2SO_4 into the CR dye solutions. The equilibrium experiments were performed at 290, 300, 310, 320, and 330 K for 20 h. After adsorption, the treated dye solution was separated from the adsorbent by centrifugation at 10,000 rpm for 5 min, and the residual CR concentration was determined by measuring the absorbance at the wavelength of 497 nm using a UV–Vis spectrophotometer (Shimadzu, Japan). Batch adsorption experiments were conducted by varying the dye concentration (500–3,000 mg/L), pH values (5.69–12.65), salt concentration (0.05–0.30 g/30 mL), and DDA (0.93%–41.48%). Each experiment was triplicated under identical condition for the purpose of reducing the random error. The equilibrium adsorption capacity Q_e (mg/g) and percentage removal (%) of CR were expressed by following formulas:

$$Q_e = \frac{(C_0 - C_e) \times V}{m} \quad (2)$$

$$\text{R emoval \%} = \frac{(C_0 - C_e)}{C_0} \times 100\% \quad (3)$$

where C_0 (mg/L) is the initial CR concentration, C_e (mg/L) is the equilibrium CR concentration, V (L) is the volume of CR solution, and m (g) is the mass of the adsorbent.

In this work, Langmuir and Freundlich models were used to study the equilibrium adsorption isotherms and the interaction between CR and the adsorbent. Langmuir model assumed a monolayer adsorption behavior on a homogeneous adsorbent surface. The equation can be described as Eq. (4):

$$Q_e = \frac{Q_m \cdot K_L \cdot C_e}{1 + K_L \cdot C_e} \tag{4}$$

where Q_e (mg/g) and Q_m (mg/g) are equilibrium adsorption capacity and maximum adsorption capacity, respectively, K_L (L/mg) is Langmuir constant related to binding energy between the adsorbate and the adsorbent, and C_e (mg/L) is the equilibrium CR concentration in the solution. Its linear form can be expressed as Eq. (5):

$$\frac{C_e}{Q_e} = \frac{C_e}{Q_m} + \frac{1}{K_L \cdot Q_m} \tag{5}$$

Freundlich model is suitable for multilayer adsorption on a heterogeneous adsorbent surface and its equation can be described as Eq. (6):

$$Q_e = K_f \cdot C_e^{1/n} \tag{6}$$

where K_f and n are Freundlich constants based on empirical evidence and related to binding energy between the adsorbate and the adsorbent. Its linear form can be expressed as Eq. (7):

$$\ln Q_e = \ln K_f + 1/n \ln C_e \tag{7}$$

2.7. Adsorption kinetics study

The adsorption kinetics study was also conducted by agitating 0.1 g of adsorbent with 30 mL of CR solution in a plastic tube using a temperature-controlled shaker at a speed of 200 rpm. The adsorption time was set from 30 min to 6 h. The experimental data were fitted by pseudo-first-order kinetic equation and pseudo-second-order kinetic equation. The pseudo-first-order equation can be expressed as:

$$\frac{dQ_t}{dt} = k_1(Q_e - Q_t) \tag{8}$$

where Q_t (mg/g) and Q_e (mg/g) are the absorbed amounts of CR on the adsorbent at time t and equilibrium, and k_1 (min^{-1}) is the pseudo-first-order rate constant. Its linear form can be given as Eq. (9):

$$\log(Q_e - Q_t) = \log Q_e - k_1 t/2.303 \tag{9}$$

The pseudo-second-order equation can be expressed as:

$$\frac{dQ_t}{dt} = k_2(Q_e - Q_t)^2 \tag{10}$$

where k_2 (g/mg/min) is pseudo-second-order rate constant. Its linear form can be given as Eq. (11):

$$\frac{t}{Q_t} = \frac{t}{Q_e} + \frac{1}{k_2 Q_e^2} \tag{11}$$

2.8. Thermodynamics study

The thermodynamic parameters, including the change of standard Gibbs free energy change (ΔG), change of standard enthalpy (ΔH), and change of standard entropy (ΔS), were calculated by the following equations:

$$\Delta G = -RT \ln K_c \tag{12}$$

$$\Delta G = \Delta H - T\Delta S \tag{13}$$

$$\ln K_c = -\frac{\Delta H}{RT} + \frac{\Delta S}{R} \tag{14}$$

$$K_c = C_s / C_e \tag{15}$$

where T is the absolute temperature of adsorption process, K_c is equilibrium constant, C_s (mg/L) is the concentration of CR adsorbed onto the adsorbent at equilibrium state and C_e (mg/L) is the concentration of CR in the solution at equilibrium state.

3. Results and discussion

3.1. Elemental analysis of chitin with different degree of deacetylation

The DDA of the chitin prepared under various deacetylation conditions is presented in Table 1. As can be seen, the DDA of CT without deacetylation was close to zero, and the DDA raised with the increase of temperature and reaction time as expected. However, it is shown from the low DDA values of CT-1, CT-2, CT-3, and CT-4 that deacetylation of the chitin from crab shells need harsh conditions. It is well known that α-chitin is the main form of chitin distributed in crabs, and due to its anti-parallel molecular chains, there is strong intermolecular hydrogen bonding [27] which hinders the permeation of OH^- into its molecule chains. Besides, the resultant sodium acetate which adhered to the chitin surface also limits the process of deacetylation reaction. The DDA of CT-5 obtained by two times of deacetylation was much higher, because the hydrogen bonding was weakened and the chitin chains got loosed after the first treatment, which made it easier for OH^- to permeate into the macromolecules.

3.2. Thermal gravimetric analysis

Figs. 1(a)–(c) show the thermogravimetric (TG) and corresponding derivative thermogravimetric (DTG) curves of CSP, CT, and CT-5. There are two major weightlessness peaks on the DTG curve of CSP (Fig. 1(a)). The first peak at 337°C was resulted from the decomposition and vaporization of chitin, and the second peak at 698°C was from the thermal decomposition of calcium carbonate. In Fig. 1(b), the only one peak at 385°C belonged to the decomposition and vaporization of chitin. From Fig. 1(c), two partially overlapping peaks at 292°C and 378°C were observed. This was attributed to the decompositions of

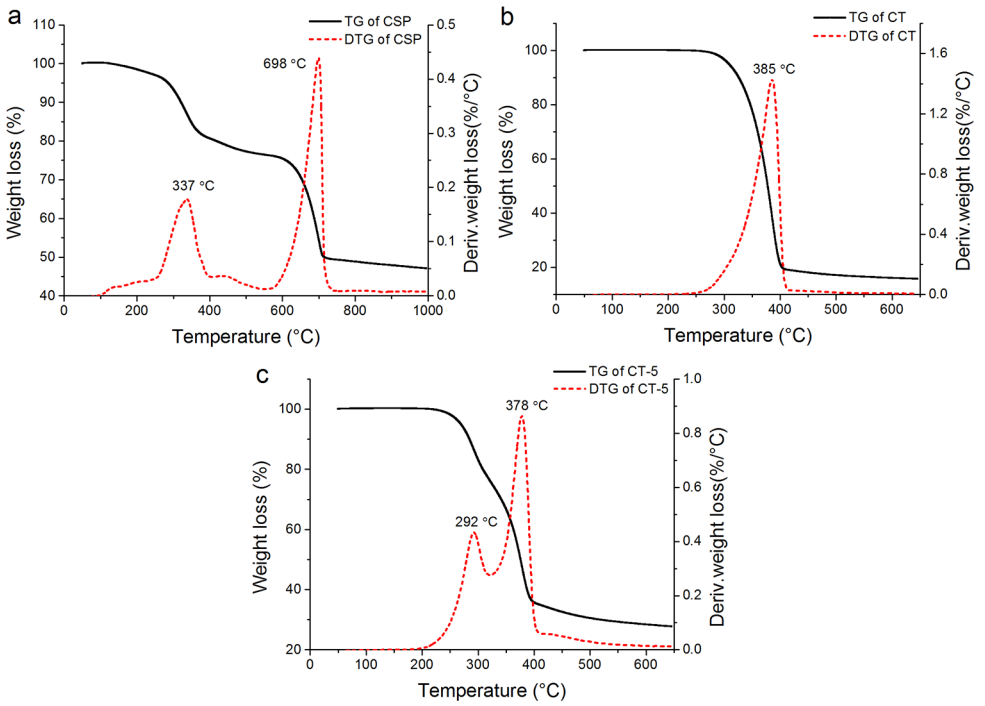

Fig. 1. TG and DTG curves of CSP (a), CT (b), and CT-5 (c).

two chitin crystals [31] composed of D-glucosamine and *N*-acetyl-D-glucosamine units, respectively. As compared with CT-5, CT presents a higher decomposition temperature because it is composed of pure *N*-acetyl-D-glucosamine units. The relatively high thermal stability of CT could be ascribed to its high crystallinity [32].

3.3. FTIR spectra of CT, CT-5, and RCT

The FTIR spectra of CT, CT-5, and CT which adsorbed Congo Red (RCT) are shown in Fig. 2. In the spectrum of CT-5, the peaks located at 3,441.38 and 3,268.75 cm^{-1} correspond to the stretching vibration of –OH and –NH. The split peaks at 1,659.38 and 1,624.59 cm^{-1} are assigned to amide I region resulted from allomorph of pure α-chitin [33]. The sharp peaks at 1,560.42 and 1,316.46 cm^{-1} are attributed to amide II and amide III regions. The peak at 2,877.46 cm^{-1} can be ascribed to the C–H stretching vibration. The presence of peaks at 1,416.30 and 1,379.32 cm^{-1} are due to $–CH_2$ and $–CH_3$ bending vibration, respectively. The peaks at 1,157.19, 1,075.44, and 1,027.35 cm^{-1} are from the asymmetrical stretching vibration and symmetrical stretching vibration of C–O–C. The spectrum of CT is similar to that of CT-5, except for the relative intensity of the peaks. Due to more amide groups on CT, the peaks at 1,659.38, 1,624.59, 1,560.42, and 1,316.46 cm^{-1} of CT are sharper than those of CT-5. As to the spectrum of RCT, the peak at 3,268.75 cm^{-1} and the band between 1,656.07 and 953.14 cm^{-1} are diminished compared with those of CT. The possible reason for the result is that the amide groups and C–O–C groups on the glucosamine ring of CT formed inter-molecular hydrogen bonds with $–NH_2$ groups on CR dye. There is no decline in the peak intensity at 3,441.38 cm^{-1} for RCT as compared with that for CT, which is different from the research of Raval et al. [34], indicating that the CR

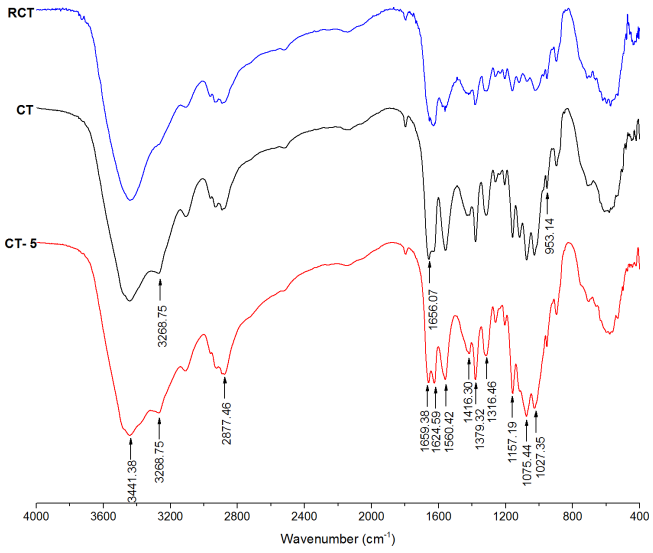

Fig. 2. FTIR spectra of CT, CT-5, and RCT.

adsorption was not associated with –OH group on CT. The –OH groups are believed to be strongly solvated in water and unable to adsorb solutes by hydrogen bonding [35].

3.4. X-ray diffraction patterns of CT and CT-5

The X-ray diffraction patterns of CT and CT-5 are presented in Fig. 3. Both of them correspond to the typical X-ray diffraction pattern of α-chitin, indicating that the structure of chitin was not destroyed in the process of extraction and deacetylation treatment. In the case of CT sample, nine main peaks were identified at 2θ = 9.35°, 19.24°, 20.75°, 23.48°,

26.39°, 27.99°, 32.25°, 34.81°, and 38.93°. For CT-5 sample, there were six evident signals on XRD pattern at 2θ = 9.37°, 19.44°, 20.81°, 23.35°, 26.26°, and 39.59°. The crystalline index of CT and CT-5 was, respectively, 75.4% and 68.3% calculated from the area method [32], showing that the crystallinity of CT-5 was lower than that of pure CT, a result in accordance with the above TGA result and relevant literatures [36].

3.5. Effect of solid–liquid ratio on adsorption

CR adsorption on the CT powder under different solid–liquid ratios is shown in Figs. 4(a) 0.1 g/30 mL and (b) 0.2 g/30 mL. It can be seen that the two adsorption curves were quite similar, indicating that the solid–liquid ratio of 0.1 g/30 mL was enough to carry out a batch of adsorption experiments. Thus, the solid–liquid ratio was chosen as 0.1 g/30 mL in the following experiments except for special illustration.

3.6. Effect of initial dye concentration

The effect of initial dye concentration (500–4,500 mg/L) on the CR adsorption onto CT was presented in Fig. 5. It can be seen that the adsorption quantity kept increasing till reaching an ultimate capacity with the increase of initial dye concentration. During the adsorption process, due to the diffusion resistance in the boundary layer of the adsorbent surface, the adsorption will reach a dynamic equilibrium when the diffusion driving force was completely offset by the diffusion resistance. As dye concentration raised, the concentration gradient between the two sides of the boundary layer increased, which led to more dye molecules permeate through the boundary layer to be adsorbed on the adsorbent. As a result, the adsorption quantity eventually increased, till saturation adsorption of CR was reached when the active sites of CT surface were fully covered. In that case, adsorption quantity remained unchanged even if dye concentration was further increased.

3.7. Effect of contact time

The CR adsorption (500 mg/L) onto CT at a series of time is shown in Fig. 6(a). It can be seen that the percentage removal of CR increased with the contact time drastically at first and then began to slow down. About 84% of CR had been adsorbed after 4 h, and the adsorption reached its equilibrium after 20 h. The maximum removal percentage of CR was obtained at 95.1%.

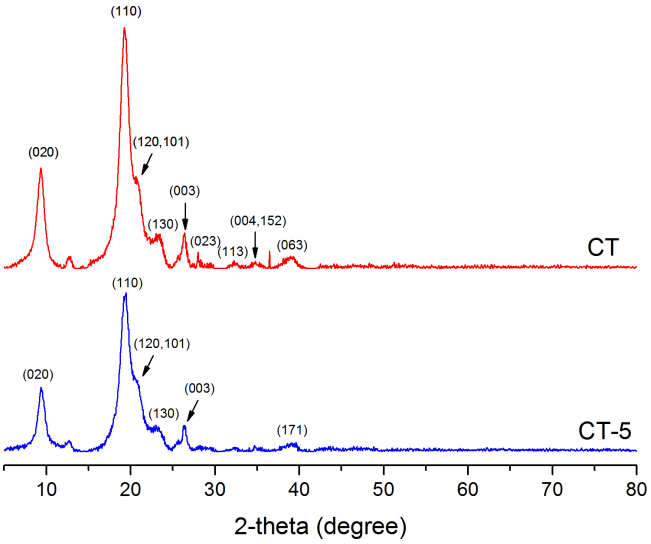

Fig. 3. X-ray diffraction patterns of CT and CT-5.

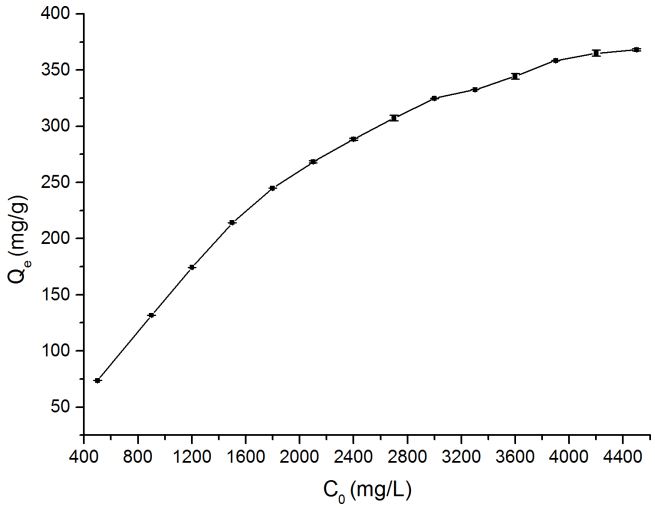

Fig. 5. Effect of initial dye concentration on CR adsorption onto CT.

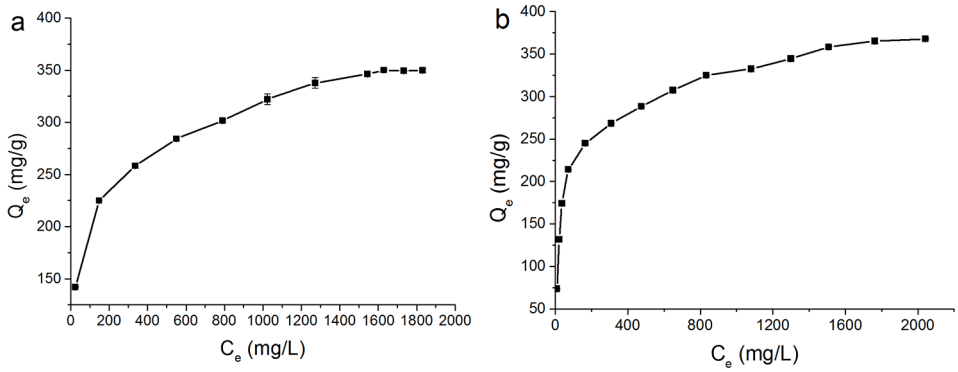

Fig. 4. Effect of solid–liquid ratio on CR adsorption onto CT: (a) 0.1 g:30 mL, (b) 0.2 g:30 mL. Conditions: pH = 7, T = 300 K, time = 20 h (Q_e: mean ± standard deviation for n = 3, the same as in the following figures unless stated specifically).

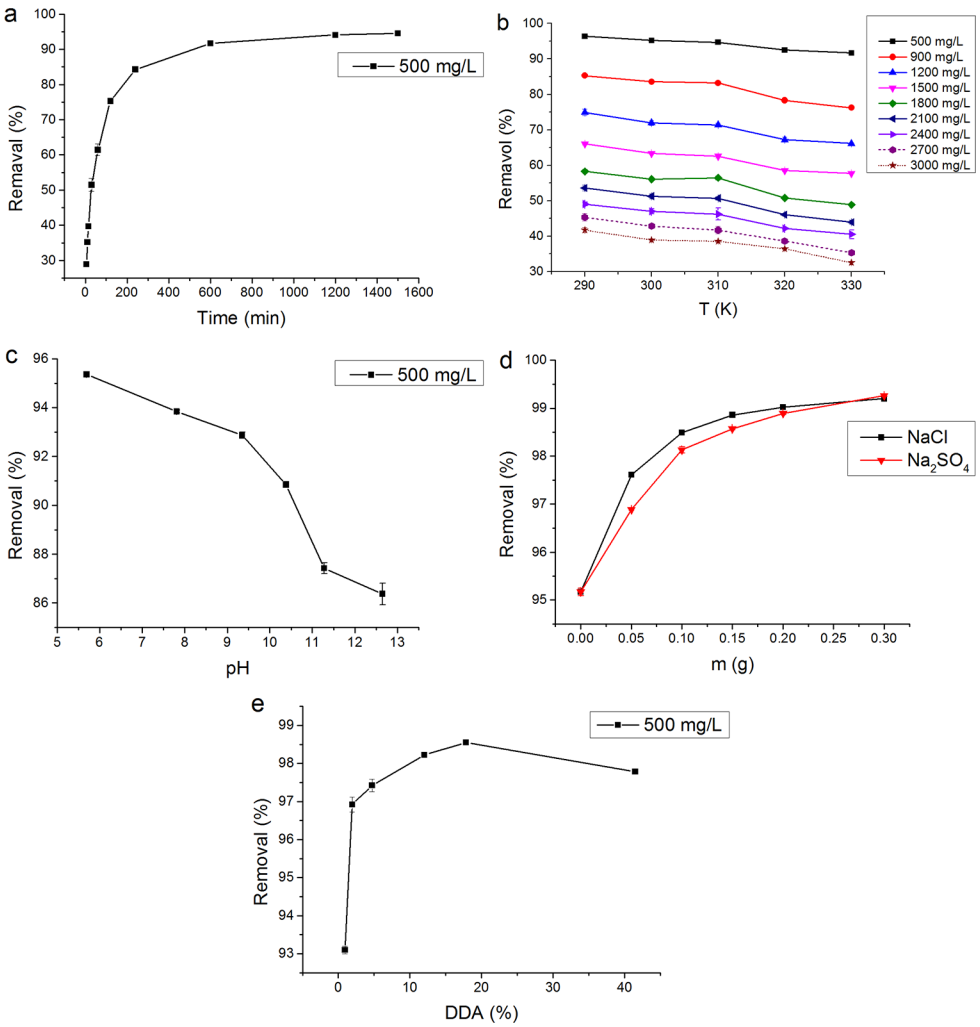

Fig. 6. Adsorption under varied conditions: (a) contact time, (b) temperature, (c) pH, (d) salt concentration, and (e) DDA.

3.8. Effect of temperature

In order to study the temperature effect on the adsorption process on CT, a batch of experiments were conducted at 290, 300, 310, 320, and 330 K, with initial dye concentration ranging from 500 to 3,000 mg/L. As shown in Fig. 6(b), the removal was decreased with the increase of temperature, which demonstrated an exothermic adsorption process adversely influenced by the rise of temperature.

3.9. Effect of pH

The pH value plays an important role in adsorption process especially for those adsorptions dominated by electrostatic interaction. In this paper, the pH effect on CR adsorption onto CT was investigated by varying the initial pH from 5.7 to 12.7 at initial dye concentration of 500 mg/L, and the results were shown in Fig. 6(c). It was found that the percentage removal decreased with the raise of pH, which can be mainly explained by electrostatic interaction. CR, a pH-sensitive anionic dye, was ionized and negatively charged in aqueous solution (in red when pH > 5.2 [37]) while CT was positively charged, in which case the adsorption is favorable. When pH increased, more and more hydroxyl ions in solution compete with dye anions for active adsorption sites, resulting in weakened electrostatic attraction between CR and CT and decreased CR removal. However, at pH = 12.7, there was still a significant removal of 86.4% observed, although the surface charge on CT became negative and the electrostatic interaction was repulsive, as the isoelectric point of CT is around the pH of 8.58 [38]. Consequently, the electrostatic interaction did not play a dominated role in CR adsorption onto CT. Combined with the results of FTIR spectra, it was concluded that CR was adsorbed onto CT mainly due to the van der Waals force and hydrogen-bonding interaction.

3.10. Effect of salt concentration

The effect of salt concentration was studied by adding different amount of NaCl or Na_2SO_4 (0.05–0.30 g) into 30 mL of 500 g/mL CR dye solution. As seen from Fig. 6(d), the removal was improved with the increase in the concentration of the two salts. NaCl and Na_2SO_4 were fully ionized in CR dye solution to produce Cl^- and SO_4^{2-}, which rejected the negatively charged CR molecules from the solution. Besides,

the addition of Cl^- and SO_4^{2-} also decreased the thickness of diffuse electric double layer on the adsorbent. As a result, CR molecules were easier to overcome the diffusion resistance to be adsorbed onto active sites of the CT surface.

3.11. Effect of degree of deacetylation

The DDA of chitin is an important factor for the adsorption performance, resulted from its effect on free amino groups, solubility, crystallinity, molecular weight, and degree of polymerization. However, the effect of chitin DDA on CR adsorption has rarely been reported. In this study, a series of chitins with different DDA (CT: 0.93%; CT-1: 1.93%; CT-2: 4.73%; CT-3: 12.02%; CT-4: 17.85%; and CT-5: 41.48%) were prepared to investigate the effect, and the results were shown in Fig. 6(e). It can be seen that CT-4 exhibited the best adsorption ability, although CT-5 has the highest DDA and the richest free amino groups. As mentioned above, the main interactions between CR and chitin were the van der Waals force and hydrogen-bonding rather than electrostatic attraction between NH_3^+ and SO_3^-, so the adsorption of CR on chitin did not depend on the content of free amino groups. At low DDA, the crystallinity of the chitin was reduced by deacetylation treatment, but when DDA reached a certain value, the chitin crystalline structure was transformed from form I to form II [31] and the crystallinity was increased on the contrary with further deacetylation. This can be supported by the fact that the crystallinity of partially deacetylation chitin is lower than that of pure chitin and pure chitosan [36]. Based on the fact that a large number of electronegative groups such as hydroxy and amide groups exist in chitin structure, there are plenty of intra- and inter-hydrogen bonds in the polymer [39]. These hydrogen bonds along with van der Waals force between molecular chains make chitin form an inerratic and orderly spiral structure and result in high crystallinity. Although deacetylation treatment reduced chitin crystallinity, crystalline region still has less possibility to adsorb CR than amorphous region because of own strong intra- and inter-molecular force. In this study, CT-4 has more amorphous regions than others, which resulted in the richer active sites on CT-4 to adsorb CR molecules through van der Waals force and hydrogen-bonding.

3.12. Orthogonal experimental design and data analysis

Orthogonal experiments in respect of time, pH, and DDA were carried out to identify the optimal adsorption condition by Taguchi method (C_0 = 500 mg/g). The orthogonal array with 25 treatment trials is shown in Table 2.

In Table 2, K_{ij} was the sum value of the removal of each contributing factor j (j = A, B, C) in level i (i = 1, 2, 3, 4, 5), and $\bar{K}_{ij}$ was the average value of the removal of each contributing factor j (j = A, B, C) in level i (i = 1, 2, 3, 4, 5), that is, and it was one fifth of K_{ij} in this study. R_j was the difference between the maximum value and the minimum value of $\bar{K}_{ij}$. The larger the value of R_j (j = A, B, C) is, the greater the effect of contributing factor j is. As can be seen from Table 2, the order of the factors in importance for adsorption was time, pH, and DDA. Since the maximum values of contributing factor j in level i were $\bar{K}_{5A}$ (97.49), $\bar{K}_{1B}$ (94.99), and $\bar{K}_{3C}$ (94.41), respectively, the best combination could be $A_5B_1C_3$. Because the optimum adsorption condition was not included in the table and the least important factor was not correct all the time, an additional experiment was carried out to verify the optimum condition. The result was shown in Table 3, which indicated that $A_5B_1C_4$ (time of 20 h, pH of 5.40, and DDA = 17.85) was the optimum adsorption condition with the CR removal of 99.28% and the maximum adsorption capacity of 148.4 mg/g.

Table 2
L_{25} (5^3) orthogonal array of three contributing factors with five levels

Experimental run	Contributing factors (j)			Removal (%)
	Time (h)	pH	DDA (%)	
	A	B	C	
1	1 (1)	1 (5.40)	1 (1.93)	83.42
2	1 (1)	2 (7.00)	2 (4.73)	77.55
3	1 (1)	3 (8.71)	3 (12.02)	86.39
4	1 (1)	4 (10.10)	4 (17.85)	83.42
5	1 (1)	5 (11.68)	5 (41.48)	68.84
6	2 (2)	1 (5.40)	2 (4.73)	95.61
7	2 (2)	2 (7.00)	3 (12.02)	95.10
8	2 (2)	3 (8.71)	4 (17.85)	95.18
9	2 (2)	4 (10.10)	5 (41.48)	90.59
10	2 (2)	5 (11.68)	1 (1.93)	66.26
11	3 (4)	1 (5.40)	3 (12.02)	98.38
12	3 (4)	2 (7.00)	4 (17.85)	97.74
13	3 (4)	3 (8.71)	5 (41.48)	96.32
14	3 (4)	4 (10.10)	1 (1.93)	87.09
15	3 (4)	5 (11.68)	2 (4.73)	80.92
16	4 (10)	1 (5.40)	4 (17.85)	99.20
17	4 (10)	2 (7.00)	5 (41.48)	97.60
18	4 (10)	3 (8.71)	1 (1.93)	95.72
19	4 (10)	4 (10.10)	2 (4.73)	95.08
20	4 (10)	5 (11.68)	3 (12.02)	93.77
21	5 (20)	1 (5.40)	5 (41.48)	98.36
22	5 (20)	2 (7.00)	1 (1.93)	97.39
23	5 (20)	3 (8.71)	2 (4.73)	97.82
24	5 (20)	4 (10.10)	3 (12.02)	98.40
25	5 (20)	5 (11.68)	4 (17.85)	95.47
K_1	399.62	474.97	429.88	–
K_2	442.74	465.38	446.98	–
K_3	460.45	471.43	472.04	–
K_4	481.37	454.58	471.01	–
K_5	487.44	405.26	451.71	–
$\bar{K}_1$	79.92	94.99	85.98	–
$\bar{K}_2$	88.55	93.08	89.40	–
$\bar{K}_3$	92.09	94.29	94.41	–
$\bar{K}_4$	96.27	90.92	94.20	–
$\bar{K}_5$	97.49	81.05	90.34	–
R_j	17.56	13.94	8.43	–

3.13. Equilibrium adsorption isotherms

The equilibrium adsorption experiments on CT were conducted at 290, 300, 310, 320, and 330 K for 20 h to ensure equilibrium attained (initial dye concentration of 500 mg/L). The adsorption isotherms were fitted by Langmuir and Freundlich models. The models were optimized by the least square method and the goodness of fitting curve was evaluated by the correlation coefficient R^2. The closer to 1 the value of R^2 is, the better fitting result is obtained. The calculated isotherm parameters at all temperatures were listed in Table 4, and the fitting results at 290 and 330 K were illustrated in Fig. 7. As can be seen, the adsorption of CR onto CT at 290 K agreed better with Freundlich isotherm, which can be confirmed by the higher value of R^2 (0.9961) for Freundlich isotherm. It indicated that the surface of CT is heterogeneous and multimolecular layer adsorption existed at low temperature. In fact, FTIR analysis proved that different function groups got involved in adsorption. Besides, physical adsorption is usually multimolecular layers adsorption because when a molecule occupies an active site, others still can combine with the site through van der Waals force or hydrogen bonds. Nevertheless, as the temperature rose, the values of R^2 for Langmuir were higher

Table 3
Determination of optimum condition for CR adsorption

Experimental run	Time (h)	pH	DDA (%)	Removal (%)
1	20	5.40	1.93	98.42
2	20	5.40	4.73	98.82
3	20	5.40	12.02	98.99
4	20	5.40	17.85	99.28
5	20	5.40	41.48	98.33

Table 4
Langmuir and Freundlich isotherms parameters for CR adsorption onto CT at different temperatures

Adsorbent	Temperature (K)	K_c	Langmuir			Freundlich		
			Q_m (mg/g)	K_L (L/g)	R^2	n	K_f (L/g)	R^2
CT	290	26.397	387.6	8.881	0.9930	4.829	81.0	0.9961
	300	19.704	366.3	8.880	0.9950	4.819	76.1	0.9914
	310	17.643	359.7	9.138	0.9961	4.800	74.7	0.9873
	320	12.259	336.7	7.298	0.9926	4.756	66.8	0.9903
	330	10.942	303.0	10.324	0.9980	5.166	70.3	0.9655

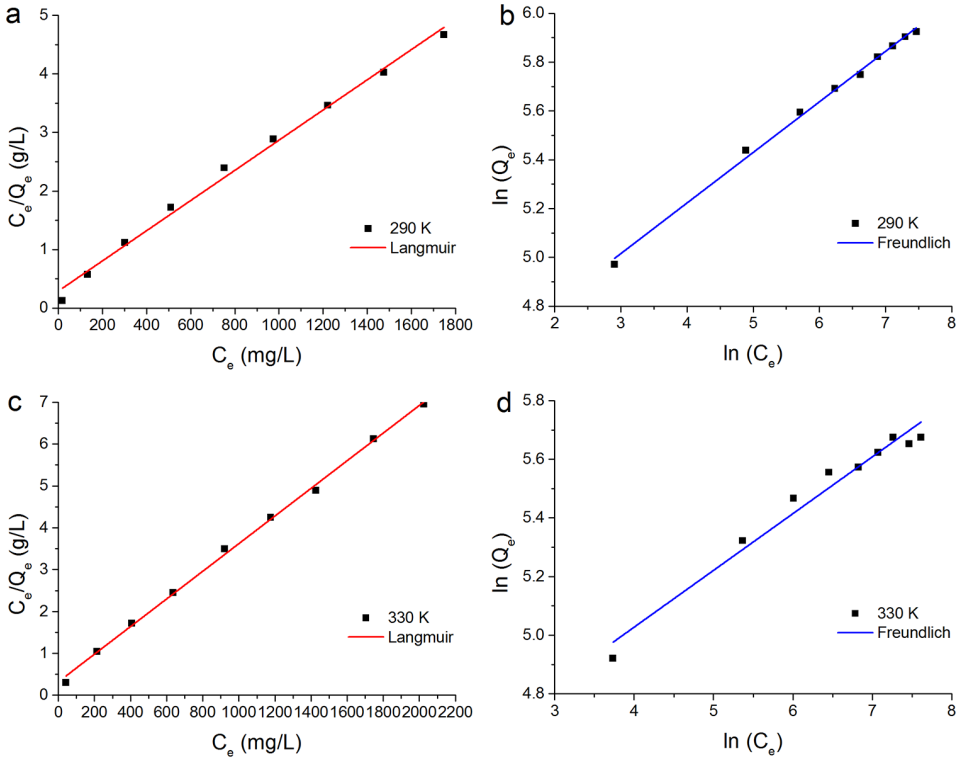

Fig. 7. Linear fitting by isotherm models: (a) Langmuir isotherm at 290 K, (b) Freundlich isotherm at 290 K, (c) Langmuir isotherm at 330 K, and (d) Freundlich isotherm at 330 K.

than those for Freundlich isotherms from 300 to 330 K, which means the equilibrium data tended to be better fitted by the Langmuir model. It was suggested that with the increase of temperature, the dye molecules adsorbed at outer layer were gradually desorbed because of molecule thermal motion, and as a result, the value of K_c and Q_m both decreased. At 330 K, the CR adsorption onto CT obeyed Langmuir isotherm well, rather than Freundlich isotherm. When compared with previously reported adsorbents (Table 5), CT in this work exhibited a relatively high adsorption performance for CR.

Table 5
Comparison between maximum adsorption capacities (Q_m) of various adsorbents calculated from Langmuir model for CR adsorption

Adsorbents	Q_m (mg/g)	References
Red mud	4.05	Namasivayam and Arasi [40]
Fly ash	4.13	Rao and Rao [41]
Sawdust	5.80	Khan et al. [15]
Kaolin	7.27	Vimonses et al. [42]
Milled tea waste	43.48	Foroughi-Dahr et al. [24]
Wheat straw	68.60	Wang et al. [43]
CTAB-TW	106.40	Foroughi-Dahr et al. [25]
Chitin beads	112.36	Raval et al. [34]
Shrimp chitin	139.00	Zúñiga-Zamora et al. [28]
Bentonite	158.70	Bulut et al. [44]
Rice hull ash	171.00	Chou et al. [45]
Activated carbon	300.00	Purkait et al. [14]
Chitosan	450.40	Chatterjee et al. [46]
CT	366.30	This work

3.14. Adsorption kinetics

Pseudo-first-order equation and pseudo-second-order equation were adopted to investigate the kinetics and mechanism of CR adsorption on CT. The model parameters calculated are listed in Table 6 and the linear fitting is shown in Fig. 8. It can be seen that the data obeyed the pseudo-second-order model ($R^2 > 0.997$) better than the pseudo-first-order model ($R^2 < 0.967$) at all initial CR concentrations. The $Q_{e,cal}$ of pseudo-second-order kinetic model was very close to the experimental data as well. It indicated that a CR molecule was adsorbed onto two active sites, which is the assumption of pseudo-second-order mechanism [47].

3.15. Adsorption thermodynamics

The thermodynamics of CR adsorption on CT was studied to investigate the energy change during the adsorption process, and the parameters were shown in Table 7. At the temperatures between 290 and 330 K, the values of ΔG were all negative, which revealed the spontaneous nature of the adsorption. Generally, ΔG value for physisorption is in the range of –20 to 0 kJ/mol, and that for chemisorption is between –80 and –400 kJ/mol [28]. Therefore, it was verified once more that CR molecules were adsorbed on CT through physical interaction, which included van der Waals force and hydrogen-bonding interaction. No evidence showed that there were sharing or exchanging of electrons between dye anions and CT adsorbent. The negative value of ΔH indicated that the adsorption process was exothermic and thus it was unfavorable for adsorption to raise the temperature. Consequently, as the temperature rose from 290 to 330 K, the equilibrium constant K_c decreased from 26.397 to 10.942. Moreover, the entropy change ΔS was negative as well, suggesting that randomness of the system was reduced during adsorption, because a great number of CR molecules were fixed on the surface of CT.

Table 6
Pseudo-first-order kinetic and pseudo-second-order kinetic parameters for CR adsorption onto CT at different initial dye concentrations

Initial concentration (mg/L)	Pseudo-first-order kinetic				Pseudo-second-order kinetic		
	$k_1 \times 10^3$ (min^{-1})	$Q_{e,cal}$ (mg/g)	$Q_{e,exp}$ (mg/g)	R^2	$k_2 \times 10^4$ (g/mg/min)	$Q_{e,cal}$ (mg/g)	R^2
500	5.988	48.5	139.1	0.9479	3.271	140.3	0.9999
900	3.938	104.3	213.9	0.9519	1.360	202.8	0.9990
1,200	3.570	125.4	247.3	0.9669	1.150	228.8	0.9975
1,800	3.478	150.5	290.2	0.9611	0.949	266.7	0.9973

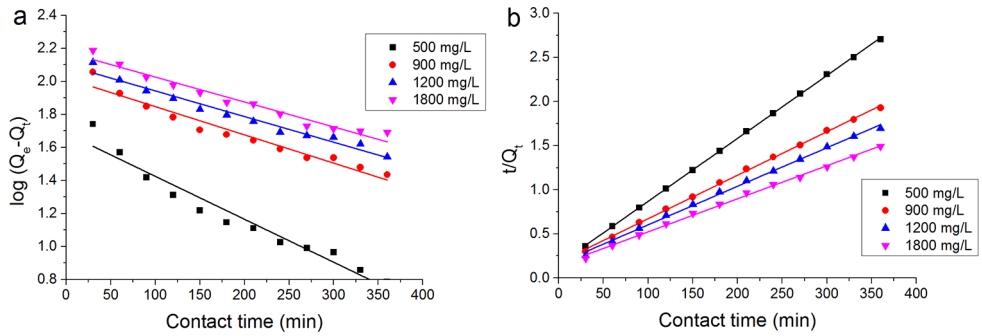

Fig. 8. Linear fitting of CR adsorption onto CT by kinetic models of (a) pseudo-first-order and (b) pseudo-second-order.

Table 7
Thermodynamic parameters for CR adsorption onto CT at different temperatures

Temperature (K)	K_c	ΔG (kJ/mol)	ΔH (kJ/mol)	ΔS (J/mol/K)
290	26.397	–7.893	–17.801	–34.2
300	19.704	–7.435		
310	17.643	–7.398		
320	12.259	–6.668		
330	10.942	–6.565		

4. Conclusions

Chitin with different DDA was prepared from crab shells waste and applied to CR adsorption. After deacetylation, both thermal stability and crystallinity of CT-5 declined compared with CT. It was revealed from adsorption experiments that the removal efficiency reached 99.28% under the optimum condition at 300 K (DDA = 17.85%, pH = 5.40, and time = 20 h). The equilibrium data agreed well with Langmuir isotherm at high temperature and the adsorption kinetics obeyed pseudo-second-order model. Multisites including amino, acetyl amino, O-glycosides, and –O– on the pyranose ring of CT were involved in the adsorption through hydrogen bonds and van der Waals force. It was further indicated from the experiment on DDA effect that the crystallinity of chitin played a more important role than amino group content in CR adsorption. Moreover, adsorption on CT was proved to a physisorption with spontaneous and exothermic nature in thermodynamic study. These results suggested that CT is a promising adsorbent for the removal of CR from dye effluents.

Symbols

C_0 — The initial CR concentration in the solution, mg/L
C_e — The equilibrium CR concentration in the solution, mg/L
Q_e — The equilibrium adsorption capacity, mg/g
Q_m — The maximum adsorption capacity, mg/g
V — The volume of CR solution, L
m — The weight of the adsorbent, g
T — The absolute temperature, K
K_L — Langmuir isotherm constant, L/g
K_f — Freundlich isotherm constant, L/g
Q_t — The absorbed amounts of CR on the adsorbent at time t, mg/g
$Q_{e,\text{cal}}$ — The equilibrium capacity calculating from Langmuir model, mg/g
$Q_{e,\text{exp}}$ — The equilibrium capacity obtained by experimental data, mg/g
k_1 — The pseudo-first-order rate constant, min^{-1}
k_2 — The pseudo-second-order rate constant, g/mg/min
K_c — The equilibrium constant
C_s — The concentration of CR adsorbed onto the adsorbent at equilibrium state, mg/L
ΔG — The change of standard Gibbs free energy, kJ/mol
ΔH — The change of standard enthalpy, kJ/mol
ΔS — The change of standard entropy, J/mol/K

References

[1] J.A. González, M.E. Villanueva, L.L. Piehl, G.J. Copello, Development of a chitin/graphene oxide hybrid composite for the removal of pollutant dyes: adsorption and desorption study, Chem. Eng. J., 280 (2015) 41–48.
[2] R.-M. Gong, M. Li, C. Yang, Y.-Z. Sun, J. Chen, Removal of cationic dyes from aqueous solution by adsorption on peanut hull, J. Hazard. Mater., 121 (2005) 247–250.
[3] T. Sismanoglu, A.Z. Aroguz, Adsorption kinetics of diazo-dye from aqueous solutions by using natural origin low-cost biosorbents, Desal. Wat. Treat., 54 (2015) 736–743.
[4] I.D. Mall, V.C. Srivastava, N.K. Agarwal, I.M. Mishra, Removal of congo red from aqueous solution by bagasse fly ash and activated carbon: kinetic study and equilibrium isotherm analyses, Chemosphere, 61 (2005) 492–501.
[5] A.K. Verma, R.R. Dash, P. Bhunia, A review on chemical coagulation/flocculation technologies for removal of colour from textile wastewaters, J. Environ. Manage., 93 (2012) 154–168.
[6] E-S.Z. El-Ashtoukhy, N.K. Amin, Removal of acid green dye 50 from wastewater by anodic oxidation and electrocoagulation—a comparative study, J. Hazard. Mater., 179 (2010) 113–119.
[7] Y.-Y. Sun, G. Wang, Q. Dong, B.-Q. Qian, Y.-L. Meng, J.-S. Qiu, Electrolysis removal of methyl orange dye from water by electrospun activated carbon fibers modified with carbon nanotubes, Chem. Eng. J., 253 (2014) 73–77.
[8] H.R. Rashidi, N.M.N. Sulaiman, N.A. Hashim, C.R.C. Hassan, M.R. Ramli, Synthetic reactive dye wastewater treatment by using nano-membrane filtration, Desal. Wat. Treat., 55 (2015) 86–95.
[9] J. Labanda, J. Sabaté, J. Llorens, Experimental and modeling study of the adsorption of single and binary dye solutions with an ion-exchange membrane adsorber, Chem. Eng. J., 166 (2011) 536–543.
[10] L. Ayed, S. Achour, E. Khelifi, A. Cheref, A. Bakhrouf, Use of active consortia of constructed ternary bacterial cultures via mixture design for congo red decolorization enhancement, Chem. Eng. J., 162 (2010) 495–502.
[11] G. Crini, P.M. Badot, Application of chitosan, a natural aminopolysaccharide, for dye removal from aqueous solutions by adsorption processes using batch studies: a review of recent literature, Prog. Polym. Sci., 33 (2008) 399–447.
[12] V.K. Garg, R. Gupta, A.B. Yadav, R. Kumar, Dye removal from aqueous solution by adsorption on treated sawdust, Bioresour. Technol., 89 (2003) 121–124.
[13] M.T. Yagub, T.K. Sen, S. Afroze, H.M. Ang, Dye and its removal from aqueous solution by adsorption: a review, Adv. Colloid Interfac., 209 (2014) 172–184.
[14] M.K. Purkait, A. Maiti, S. Dasgupta, S. De, Removal of congo red using activated carbon and its regeneration, J. Hazard. Mater., 145 (2007) 287–295.
[15] T.A. Khan, S. Sharma, E.A. Khan, A.A. Mukhlif, Removal of congo red and basic violet 1 by chir pine (*Pinus roxburghii*) sawdust, a saw mill waste: batch and column studies, Toxico. Enviro. Chem., 96 (2014) 555–568.
[16] S.T. Ong, C.K. Lee, Z. Zainal, Removal of basic and reactive dyes using ethylenediamine modified rice hull, Bioresour. Technol., 98 (2007) 2792–2799.
[17] W.-X. Zhang, H. Yan, H.-J. Li, Z.-W. Jiang, L. Dong, X.-W. Kan, H. Yang, A.-M. Li, R.-S. Cheng, Removal of dyes from aqueous solutions by straw based adsorbents: batch and column studies, Chem. Eng. J., 168 (2011) 1120–1127.
[18] M. Shirzad-Siboni, S.J. Jafari, O. Giahi, I. Kim, S.M. Lee, J.K. Yang, Removal of acid blue 113 and reactive black 5 dye from aqueous solutions by activated red mud, J. Ind. Eng. Chem., 20 (2014) 1432–1437.

[19] J.-X. Lin, S.-L. Zhan, M.-H. Fang, X.-Q. Qian, H. Yang, Adsorption of basic dye from aqueous solution onto fly ash, J. Environ. Manage., 87 (2008) 193–200.
[20] M.V. Sureshkumar, C. Namasivayam, Adsorption behavior of direct red 12B and rhodamine B from water onto surfactant-modified coconut coir pith, Colloid. Surface. A., 317 (2008) 277–283.
[21] B. Meroufel, O. Benali, M. Benyahia, Y. Benmoussa, M.A. Zenasni, Adsorptive removal of anionic dye from aqueous solutions by Algerian kaolin: characteristics, isotherm, kinetic and thermodynamic studies, J. Mater. Environ. Sci., 4 (2013) 482–491.
[22] M. Toor, B. Jin, Adsorption characteristics, isotherm, kinetics, and diffusion of modified natural bentonite for removing diazo dye, Chem. Eng. J., 187 (2012) 79–88.
[23] C.-S. Shen, Y. Shen, Y.-Z. Wen, H.-Y. Wang, W.-P. Liu, Fast and highly efficient removal of dyes under alkaline conditions using magnetic chitosan-Fe(III) hydrogel, Water Res., 45 (2011) 5200–5210.
[24] M. Foroughi-Dahr, H. Abolghasemi, M. Esmaili, A. Shojamoradi, H. Fatoorehchi, Adsorption characteristics of congo red from aqueous solution onto tea waste, Chem. Eng. Commun., 202 (2015) 181–193.
[25] M. Foroughi-Dahr, H. Abolghasemi, M. Esmaieli, G. Nazari, B. Rasem, Experimental study on the adsorptive behavior of congo red in cationic surfactant-modified tea waste, Process Saf. Environ., 95 (2015) 226–236.
[26] C.K.S. Pillai, W. Paul, C.P. Sharma, Chitin and chitosan polymers: chemistry, solubility and fiber formation, Prog. Polym. Sci., 34 (2009) 641–678.
[27] I. Hamed, F. Özogul, J.M. Regenstein, Industrial applications of crustacean by-products (chitin, chitosan, and chitooligosaccharides): a review, Trends. Food Sci. Tech., 48 (2016) 40–50.
[28] A. Zúñiga-Zamora, J. García-Mena, E. Cervantes-González, Removal of congo red from the aqueous phase by chitin and chitosan from waste shrimp, Desal. Water Treat., 57 (2016) 14674–14685.
[29] D.S.P. Franco, J.S. Piccin, E.C. Lima, G.L. Dotto, Interpretations about methylene blue adsorption by surface modified chitin using the statistical physics treatment, Adsorption, 21 (2015) 557–564.
[30] S. Kaur, G.S. Dhillon, Recent trends in biological extraction of chitin from marine shell wastes: a review, Crit. Rev. Biotechnol., 35 (2015) 44–61.
[31] R.J. Samuels, Solid state characterization of the structure of chitosan films, J. Polym. Sci. Pol. Phys., 19 (1981) 1081–1105.
[32] M. Jaworska, K. Sakurai, P. Gaudon, E. Guibal, Influence of chitosan characteristics on polymer properties. I: Crystallographic properties, Polym. Int., 52 (2003) 198–205.
[33] S. Dhananasekaran, R. Palanivel, S. Pappu, Adsorption of methylene blue, bromophenol blue, and boomassie brilliant blue by α-chitin nanoparticles, J. Adv. Res., 7 (2016) 113–124.
[34] N.P. Raval, P.U. Shah, D.G. Ladha, P.M. Wadhwani, N.K. Shah, Comparative study of chitin and chitosan beads for the adsorption of hazardous anionic azo dye congo red from wastewater, Desal. Water Treat., 57 (2016) 9247–9262.
[35] C.H. Giles, A.S.A. Hassan, Adsorption at organic surfaces V—A Study of the adsorption of dyes and other organic solutes by cellulose and chitin, J. Soc. Dyers. Colour., 74 (1958) 846–857.
[36] K. Ogawa, T. Yui, Crystallinity of partially N-acetylated chitosans, Biosci. Biotech. Bioch., 57 (1993) 1466–1469.
[37] M. Johansson, I. Synnerstad, L. Holm, Acid transport through channels in the mucous layer of rat stomach, Gastroenterology, 119 (2000) 1297–1304.
[38] P. Liu, H. Sehaqui, P. Tingaut, A. Wichser, K. Oksman, A.P. Mathew, Cellulose and chitin nanomaterials for capturing silver ions (Ag^+) from water via surface adsorption, Cellulose, 21 (2014) 449–461.
[39] D. Carlstrom, The crystal structure of α-chitin (poly-N-acetyl-D-glucosamine), J. Biophys. Biochem. Cytol., 3 (1957) 669–683.
[40] C. Namasivayam, D.J.S.E. Arasi, Removal of congo red from wastewater by adsorption onto waste red mud, Chemosphere, 34 (1997) 401–417.
[41] V.V.B. Rao, S.R.M. Rao, Adsorption studies on treatment of textile dyeing industrial effluent by flyash, Chem. Eng. J., 116 (2006) 77–84.
[42] V. Vimonses, S.-M. Lei, B. Jin, C.W.K. Chow, C. Saint, Adsorption of congo red by three Australian kaolins, Appl. Clay Sci., 43 (2009) 465–472.
[43] Z.-W. Wang, P. Han, Y.-B. Jiao, D. Ma, C.-C. Dou, R.-P. Han, Adsorption of congo red using ethylenediamine modified wheat straw, Desal. Water Treat., 30 (2011) 195–206.
[44] E. Bulut, M. Özacar, İ.A. Şengil, Equilibrium and kinetic data and process design for adsorption of congo red onto bentonite, J. Hazard. Mater., 154 (2008) 613–622.
[45] K.S. Chou, J.C. Tsai, C.T. Lo, The adsorption of congo red and vacuum pump oil by rice hull ash, Bioresource Technol., 78 (2001) 217–219.
[46] S. Chatterjee, M.W. Lee, S.H. Woo, Adsorption of congo red by chitosan hydrogel beads impregnated with carbon nanotubes, Bioresource Technol., 101 (2010) 1800–1806.
[47] A.B. Pérez-Marín, V.M. Zapata, J.F. Ortuño, M. Aguilar, J. Sáez, M. Lloréns, Removal of cadmium from aqueous solutions by adsorption onto orange waste, J. Hazard. Mater., 139 (2007) 122–131.